Barbara Nasiłowska, Zdzisław Bogdanowicz, Janusz Terpiłowski, Krzysztof Pańcikiewicz

Thermophysical properties of 904L austenitic steel

Właściwości cieplnofizyczne stali austenitycznej 904L

Abstract

This paper presents the results of the structural investigations and thermophysical properties of 904L steel parent material. Experimental studies on the structure of 904L steel proved a pure austenitic structure. Both the experimental research and analysis of the thermophysical properties of 904L steel were complemented with the results of the thermal conductivity calculations for the tested material. The paper presents a brief description of the measurements, the procedures for evaluating the data, and a set of the obtained results.

Keywords: thermophysical properties, steel 904L, specific heat, thermal diffusivity, thermal conductivity, specific heat

Streszczenie

W pracy przedstawiono wyniki badań strukturalnych i właściwości cieplnofizyczne materiału rodzimego stali 904L. Badania eksperymentalne struktury stali 904L wykazały strukturę czysto austenityczną. Badania doświadczalne i analizę właściwości cieplnofizycznych stali 904L uzupełniono wynikami obliczeń przewodności cieplnej badanego materiału. W pracy przedstawiono zwięzły opis wykonywanych pomiarów, charakterystykę procedur opracowania danych oraz komplet uzyskanych wyników.

Słowa kluczowe: właściwości cieplnofizyczne, stal 904L, ciepło właściwe, dyfuzyjność cieplna, przewodność cieplna, ciepło właściwe

1. Introduction

The mechanical and thermophysical properties of 904L steel accounting for its work in high temperatures, resistance to corrosion, and resistance to low-cycle thermal fatigue result in the fact that this steel is mainly used to produce chemical installations in nuclear power plants (e.g., FLAMANVILLE in France) [1] and also to produce the inside walls of manholes that are constantly in direct contact with hazardous substances.

Barbara Nasiłowska, Zdzisław Bogdanowicz: Military University of Technology, Institute of Optoelectronics, Warsaw, Poland, **Janusz Terpiłowski:** Military University of Technology, Faculty of Mechatronics and Aerospace, Warsaw, Poland, **Krzysztof Pańcikiewicz:** AGH University of Science and Technology, Department of Physical and Powder Metallurgy, Krakow, Poland; barbara.nasilowska@wat.edu.pl

In his report of 2014, Watson [2] stated that material loss, dents, and fractures were the main reasons for the pipeline failures in Canada; however, according to the Federal Pipeline and Hazardous Materials Safety Administration, the most frequent reasons for industry pipeline failures in the USA during the years of 2013–2014 were constructional faults and the corrosion developed on the inside walls of the installations [2].

Under the influence of load and temperature, changes in the thermophysical properties of austenitic steel material can occur.

The design of chemical structures requires any necessary information concerning the thermal properties of a material from the designer.

Specific heat is a mass unit known as the thermal capacity of a certain specific quantity of material [3–5]. Specific heat depends on the conditions under which the measurement is taken; e.g., specific heat can be measured under constant pressure conditions (denoted by c_p) or under constant capacity conditions (denoted by c_v) [5].

In the case of a solid body, it is much easier to measure specific heat under constant pressure than at a constant capacity. This results from the fact that, during the delivery of thermal energy to a specimen (which is a solid body), it is much easier to sustain the specimen under constant pressure conditions than to prevent a change in its capacity [5].

Rempe and Knudson determined the density functions [kg·m^{-3}], specific heat capacity [J·kg^{-1}·K^{-1}], thermal diffusivity [cm^2·s^{-1}], and thermal conductivity [W·m^{-1}·K^{-1}] for low-carbon steel SA533-B1, stainless steel 304 and Inconel 600 within a temperature range of 0–1400°C. The presented results of the investigations demonstrated a constant change of function within a temperature range of 740–840°C [6].

In a conference article, Duthil presented the tests results of specific heat for metals (e.g., Cu, Al, Ti, austenitic steel 304L, Cu-Ni, and Cu-Mn alloys) as well as for He and N$_2$ gases. The properties of the materials depended on their chemical composition, structure, atomic interactions, etc. as well as temperature changes [7].

The free energy (G) per unit volume of a phase or combination of phases is defined in terms of other thermodynamic parameters such as enthalpy or heat content (H), absolute temperature (T), and entropy (S) as follows [8]:

$$G = H - TS \tag{1}$$

Enthalpy is the total energy of the phase (or microstructure composed of several phases) per unit volume of that structure. Entropy is the measure of the degree of order associated with a given structure at a given temperature. It may be influenced by the amplitude of the atomic vibrations, the mixing of several component types of atoms and vacant lattice sites in a given phase, or the degree of order associated with a given solid or liquid structure [8, 9].

Several publications, including works [6, 7] and standards [10, 11], are dedicated to the thermal properties typical for austenitic steel of series 300. However, the current state of the literature lacks the experimental results of tests on the thermophysical properties of 940L steel applicable to the chemical and refinery industry. The thermophysical

information of 904L steel is necessary for designing chemical installations, whereas enthalpy and entropy are applied to the model phase transitions in the structure.

2. Experimental research

Structural tests of 904L austenitic steel were carried out with the use of a Nicon 200 light microscope and a Quanta 3D FEG scanning electron microscope using an FSD (Forward Scatter Detector) and EDSD (Electron Backscatter Diffraction).

An equilibrium system of 904L steel (temperature 0–1500°C) was developed based on its chemical composition in Thermo-Calc software.

Research on the thermo-physical properties of 904L austenitic steel was conducted, with the use of a method described in [12] at the Institute of Aviation Technology – Department of Aerodynamics and Thermodynamics, Faculty of Mechatronics and Aerospace, Military University of Technology in Poland.

Investigations of the thermal diffusivity were carried out with a method of surface impulse heating with a differential measurement of temperatures on flat surfaces of the tested disk specimen cut out with an electrical discharge machine. The dimensions of the specimens are listed in Table 1.

Table 1. Dimensions of specimens cut out with electrical discharge machine to investigate specific heat and diffusivity of 904L steel

Tested parameter	Symbol	Dimensions [mm]		Temperature range of tests	
		outer diameter	height	[°C]	[K]
Specific heat	$c_p(t)$	5.0	0.5	−20–420	253.15–693.15
Thermal diffusivity	$\alpha(T)$	12.0	2.0	20–870	293.15–1143.15

Specific heat was defined based on the results of the experimental studies within a temperature range of 253.15–693.15K.

$$c_p(T) = 452.0306 + 0.3101 \cdot T - 0.0004 \cdot T^2 + 2.2033 \cdot 10^{-7} \cdot T^3 \quad \text{J} \cdot \text{kg}^{-1} \cdot \text{K}^{-1} \quad (2)$$

To measure the thermal diffusivity of 904L steel, there a modified impulse method [12] developed at the Military University of Technology was used (described in [13, 14]), which applies the same model of heat exchange that is applied in Parker's method. The procedure to determine the thermal diffusivity with a modified impulse method consists of the following steps:

– generating a surface source of heat (flash lamp, impulse laser) on the surface of a front flat and parallel adiabatic specimen and recording (starting from this moment) the changes of temperature differences $\Delta\Theta(t) = T1(t) - T2(t)$ between a front and rear surface of the tested specimen;

- obtaining a theoretical solution to this problem in the form of the change of temperature differences on the extreme surfaces of the specimen $\Delta\Theta(t) = T1(t) - T2(t)$;
- identifying an appropriate curve from a set that is a theoretical solution to this problem with an experimental curie, while the parameter subjected to a change in the identification process is the value of thermal diffusivity.

The results of the comparative studies of determining the thermal diffusivity with a modified impulse method and with Parker's method presented in [12, 13] proved that the first of these methods provides much more accurate measurements. The total measurement error (taking into account the influence of heat loss from both specimen surfaces, measurement error of its thickness, and fluctuations of measurement signal resulting from thermal noises and outside electromagnetic interference) was estimated to be less than 3% in the case of the modified impulse method, whereas this is equal to 10% for the classical Parker's method.

A flow chart of the stand for thermal diffusivity measurement is presented in Figure 1. The special design of the specimen holder as well as the 10^{-4} Pa vacuum maintained in the stove were aimed at minimizing heat loss to the environment through convection and conductivity. A neodymium laser was applied as an impulse source of heat. The duration of a laser impulse is less than 1 ms, and its energy can be changed within a range of 5–15 J, while the radiation beam diameter is approximately 14 mm (Fig. 2).
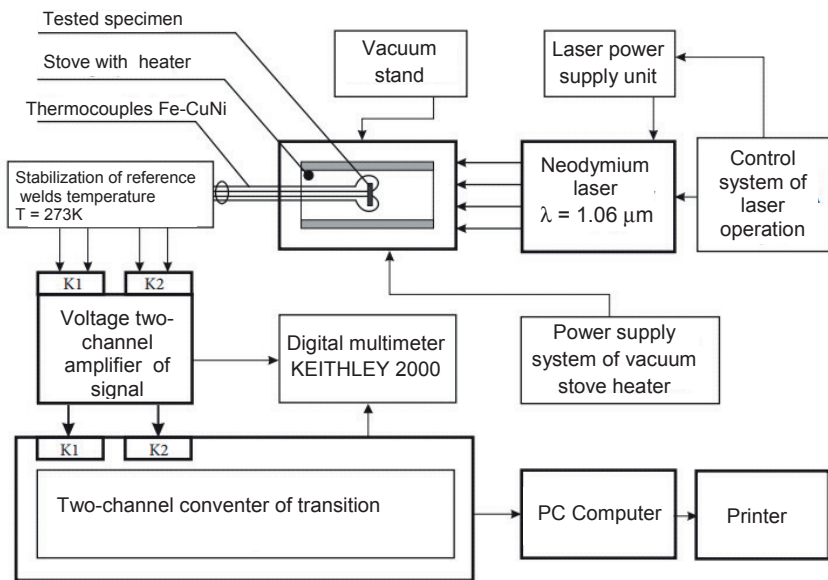

Fig. 1. Flow chart of stand for measurement of heat diffusivity for solid bodies [12, 13]
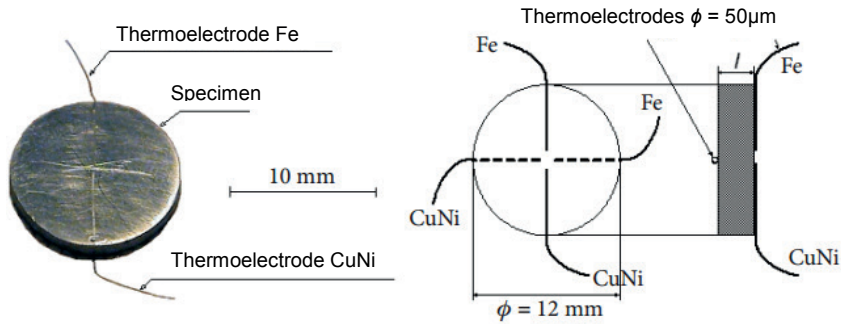
Fig. 2. General view of tested specimen together with thermoelectrodes welded to its front surface as well as its dimensions [13]

Figure 2 presents a general view of a sample specimen together with thermoelectrodes welded to its surface; these were necessary to measure the fixed temperature of the specimen just before a shot from the laser into its face surface as well as changes in the temperature differences on its extreme surfaces just after a shot from the laser. In this case, elements of a J (Fe-CuNi) type were used to measure the temperature.

Determining the thermal diffusivity value of the tested specimen took place as a result of an identification process of a relative curve from a set of theoretical solutions with experimental proceedings using computer software.

The investigations of specific heat were conducted with the use of a Perkin-Elmer Pyris scanning microcalorimeter adopted to carry out thermal analyses. The application of a heat flux compensation method as a principle of thermal signal acquisition gives privilege to this device in specific heat measurements [13]. The measurements were conducted on specimens of 8 mm·g^{-1} mass each. The device was calibrated for both the temperature measurements and investigations of the thermal effects using standard calibration procedures. Indium and zinc were used as the standards. The calibration was performed for speeds (pace) of temperature changes of 10 K·min^{-1}. Information about the reference of the signal was applied to the tests of the thermal characteristics of the scanning process. In calorimetric terminology, this means taking into account a baseline curve shape. This curve was recorded under the conditions accurately corresponding to a basic measurement with empty measurement chambers covered with standard platinum lids. Sustaining the same conditions means conducting the measurement at the same standard velocity of inert gas (dehydrated gas N$_2$) with a flow equal to 20 ml·min^{-1}, with a protective heater of the head turned on and after stabilizing the parameters of the head operation under the conditions of cooling by a Perkin-Elmer Intracooler cooler. To determine the specific heat, a more precise method for the experimental determination of thermal capacity (namely, the three curves method) was applied [12, 13]. This is a method of a comparative (relative) measurement.

3. Research object

The object of the research is 904L austenitic steel (904L, UNS N08904). Its chemical composition and mechanical properties according to standard [10] and delivery certificate 2050301-FR are given in Tables 2 and 3.

Table 2. Percentage of elements in austenitic steel 904L according to delivery certificate 2050301-FR

904L	C	Mn	Si	P	S	Cr	Ni	Cu	Nb	Co	N	Mo
PN-EN 10088-1: 2014-12 [10]	≤0.02	≤2.0	≤0.7	≤0.03	≤0.01	19.0–21.0	24.0–26.0	1.20–2.00	≤0.02	≤2.0	–	–
2050301-FR	0.01	1.38	0.30	0.021	0.001	19.77	24.15	0.016	0.01	1.38	0.016	0.30

Table 3. Mechanical properties of austenitic steel 904L according to delivery certificate 205030-FR

Temperature [°C]	$R_{0.2}$ [MPa]	$R_{1.0}$ [MPa]	R_m [MPa]	A_5	HRB
+20	240	270	530–720	40	90
+400	125	155	360	–	–

4. Structure of austenitic steel 904L

Structural tests of the 904L austenitic steel demonstrated a visible grain structure with numerous twins of recrystallization nucleating on the boundaries of the grains (which is indicated by arrows in Figure 3a).
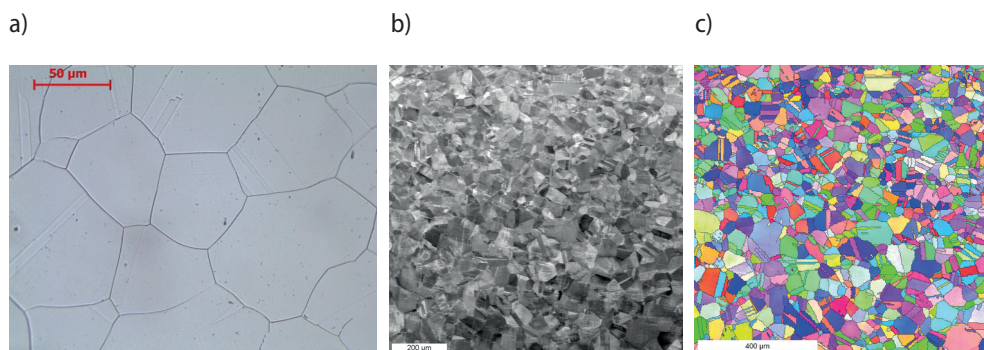
a)

b)

c)

Fig. 3. Structure of parent material of 904L austenitic steel illustrated with use of Nicon MA200 light microscope (a) as well as with use of local crystallographic orientations of scanning microscope in FSD image (b) and in EBSD image (c)

These results were verified with EBSD tests with the use of a scanning microscope. These tests also demonstrated a pure austenitic structure without any residual ferrite or carbides.

An equilibrium system of the 904L at temperatures of 0–1500°C (273–1773K) depending on the nickel content and other elements of the steel content (Fe ≤ 49, Cr 19–21, Mo 4–5, Cu 1.2–2.0, Mn ≤ 2.0, N ≤ 0.15, Si ≤ 0.7, P ≤ 0.030, S ≤ 0.010, C ≤ 0.02) was developed in the Thermo-Calc software. Based on this equilibrium system, the domination of austenite γ was proven; however, with the possibility of the occurrence of minimal quantities of phase σ (e.g., $Fe_{52}Cr_{48}$), P (e.g., Cr_3P), Laves phases (e.g., Fe_2Nb), chrome carbides (e.g., $Cr_{23}C_6$), and residual ferrite α (Fig. 4).
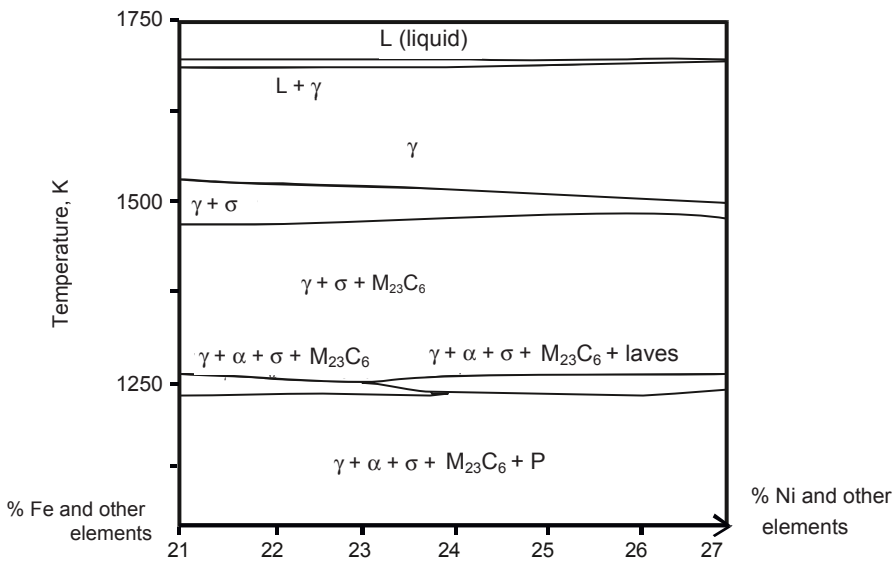

Fig. 4. Equilibrium system of 904L steel with changing nickel content

In the case when a ratio of the atomic radii of two elements A (Cr) and B (Mo, Fe, Mn) is within a range of 1.05–1.68, then Laves phases of the AB_2 type found among others in alloys of Fe, Mn, Cr, and Mo with other metals can form. Tests with the use of the SE (Secondary Electron) detector, EDS (Energy Dispersive Spectroscopy), and EBSD (Electron Backscatter Diffraction) carried out with a scanning electron microscope did not prove the presence of σ, P, or Laves phases (Fig. 5c). An analysis of the Kikuch line grid and a full scan of the surfaces of the metallographic specimens of the tested welded elements performed with the EBSD detector demonstrated pure austenite (Fig. 5).
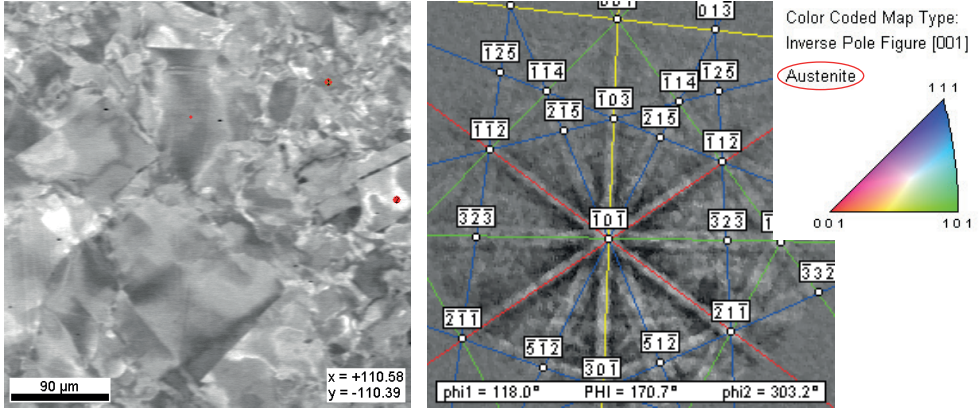
Fig. 5. Representative results of analysis of Kikuch line grid pointing to grains of pure austenite

5. Thermophysical properties of 904L austenitic steel

The thermal diffusivity $\alpha(T)$ of the 904L steel as a function of temperature changes from −20° to −900°C (253–1173K) was approximated with Relationship (3):

$$\alpha(T) = (3.133 + 0.0024\,T) \cdot 10^{-6} \; \mathrm{m}^2 \cdot \mathrm{s}^{-1} \tag{3}$$

The specific heat $c_p(T)$ was determined within a temperature range of −20–425°C (253–698K); the following relationship was obtained:

$$c_p(T) = 452.0306 + 0.3101 \cdot T - 0.0004 \cdot T^2 + 2.2033 \cdot 10^{-7} \cdot T^3 \; \mathrm{J} \cdot \mathrm{kg}^{-1} \cdot \mathrm{K}^{-1} \tag{4}$$

Also, the thermal conductivity $\lambda(T)$ of the 904L steel was determined based on the following formula:

$$\lambda(T) = \alpha(T) \cdot c_p(T) \cdot r(T) \tag{5}$$

where:
   ρ – density of 904L steel,
   $c_p(T)$ – specific heat [J·kg^{-1}·K^{-1}],
   $\alpha(T)$ – thermal diffusivity [m^2·s^{-1}].

After substituting Relationships (3) and (4) in (5) and assuming that $\rho(T) = \mathrm{const} \cong$ 8000 kg·m^{-3}, the following relationship was obtained:

$$\lambda(T) = 11.3297 + 0.016451 \cdot T - 4 \cdot 10^{-6} T^2 - 0.00216 \cdot 10^{-6} \cdot T^3 + 4.23 \cdot 10^{-12} \cdot T^4 \; \mathrm{W} \cdot \mathrm{m}^{-1} \cdot \mathrm{K}^{-1} \tag{6}$$

Since the thermal conductivity $\lambda(T)$ of the 904L steel was determined indirectly from Relationship (5) and the specific heat $c_p(T)$ was determined experimentally within the

ranges of temperature changes of −20–425°C (253–698K), the same range of temperature changes was also applied while calculating the thermal conductivity from Relationship (6) (Fig. 6). The temperatures in the expressions of these values were in the Celsius scale.
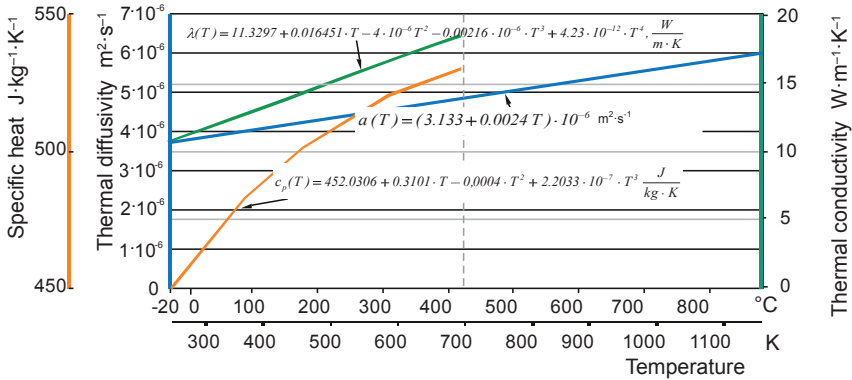

In the figure, the following equations appear:

$$\lambda(T) = 11.3297 + 0.016451 \cdot T - 4 \cdot 10^{-6} \, T^2 - 0.00216 \cdot 10^{-6} \cdot T^3 + 4.23 \cdot 10^{-12} \cdot T^4, \ \frac{W}{m \cdot K}$$

$$a(T) = (3.133 + 0.0024 \, T) \cdot 10^{-6} \ \ m^2 \cdot s^{-1}$$

$$c_p(T) = 452.0306 + 0.3101 \cdot T - 0,0004 \cdot T^2 + 2.2033 \cdot 10^{-7} \cdot T^3 \ \ \frac{J}{kg \cdot K}$$

Fig. 6. Thermal conductivity λ(T), specific heat c_p(T), and thermal diffusivity α(T) of 904L steel as function of temperature

The experimentally defined course of the thermal diffusivity (Fig. 6) in the temperature range adopted for the research reflects an actual and homogenous (pure austenitic) structure of the specimen material [12].

The enthalpy and entropy of the 904L austenitic steel as a function of temperature were determined in the Thermo-Calc software (in collaboration with AGH University of Science and Technology in Krakow). Based on chemical composition [10], two ranges of functions were defined taking into account the transition from a solid state to a liquid state, which occurs in temperature of approximately 1400°C (1680K) (Fig. 7).
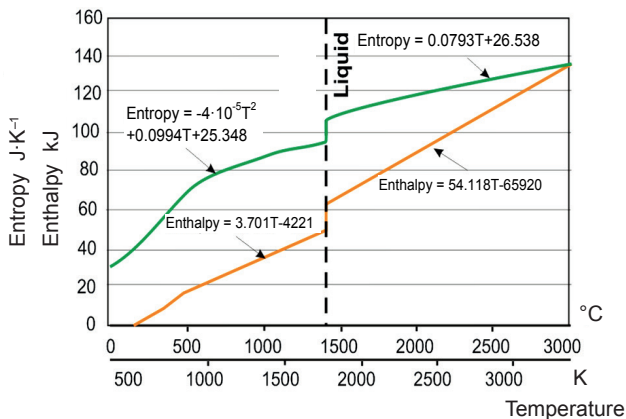

In the figure, the following equations appear:

Entropy = 0.0793T+26.538

Entropy = -4·10⁻⁵T²+0.0994T+25.348

Enthalpy = 54.118T-65920

Enthalpy = 3.701T-4221

Fig. 7. Enthalpy and entropy of 904L steel as function of temperature

The obtained results proved an entropy and enthalpy increase along with a temperature increase.

The experimental research of the thermal conductivity, specific heat, and thermal diffusivity as well as the entropy and enthalpy allowed us to improve the accuracy of the numerical calculations of the 904L austenitic steel, especially for the operation of the designed devices under conditions of increased temperatures.

6. Summary

As a result of metallographic tests that included chemical composition and microstructure analysis (using a scanning electron microscope with EBSD, FSD, and BSE detectors) as well as tests for ferrite content (using a feritscope), only pure austenite was observed without any admixture of phases and carbides.

The thermal diffusivity of 904L austenitic steel within a temperature range of room temperature to approximately 900°C (1173K) increases along with its increase from approximately $3.7 \cdot 10^{-6}$ m²·s⁻¹ to approximately $6 \cdot 10^{-6}$ m²·s⁻¹.

Changes in the specific heat and thermal conductivity within the temperature change range of −20–425°C (253–698 K) included $450\,\text{J}\cdot\text{kg}^{-1}\cdot\text{K}^{-1} \leq c_p(T) \leq 530\,\text{J}\cdot\text{kg}^{-1}\cdot\text{K}^{-1}$ and $13.0\,\text{W}\cdot\text{m}^{-1}\cdot\text{K}^{-1} \leq \lambda(T) \leq 17.6\,\text{W}\cdot\text{m}^{-1}\cdot\text{K}^{-1}$ respectively.

However, the entropy and enthalpy of the 904L austenitic steel were within the following ranges:
  − in the solid state (0–1400°C, 273–1773K)

$$30\,\text{J}\cdot\text{K}^{-1} \leq \text{entropy}\,(T) \leq 100\,\text{J}\cdot\text{K}^{-1}$$
$$-10\,\text{kJ} \leq \text{enthalpy}\,(T) \leq 50\,\text{kJ}$$

  − in the liquid state (1400–3000°C, 1773–3273K)

$$110\,\text{J}\cdot\text{K}^{-1} \leq \text{entropy}\,(T) \leq 130\,\text{J}\cdot\text{K}^{-1}$$
$$60\,\text{kJ} \leq \text{enthalpy}\,(T) \leq 130\,\text{kJ}$$

Reference

[1] Nasiłowska B.: Trwałość zmęczeniowa i przebieg pękania połączeń spawanych stali austenitycznej 1.4539 wykonanych metodą TIG i laserowo. PhD dissertation, Wojskowa Akademia Techniczna, Warszawa 2016

[2] National Energy Board: Pipeline Performance Measures. 2013 Data report. October 2014

[3] Kalinowski E.: Termodynamika. Wydawnictwo Politechniki Wrocławskiej, Wrocław 1994

[4] Szargut J.: Termodynamika techniczna. Wydawnictwo Politechniki Śląskiej, Gliwice 2000

[5] Więckowski J.: Właściwości cieplne i magnetyczne wybranych związków kobaltu o strukturze warstwowej. PhD dissertation, PAN-IF, Warszawa 2013

[6] Rempe J.L., Knudson D.L.: High temperature thermal properties for metals used in LWR vessels. Journal of Nuclear Materials, 372, 2–3 (2008), 350–357

[7] Duthil P.: Material Properties at Low Temperature. In: CAS – CERN Accelerator School: Course on Superconductivity for Accelerators, Erice, Italy, 24 April – 4 May 2013, edited by R. Bailey, 77–95

[8] Krauss G.: Steels: Processing, Structure, and Performance. Second Edition, ASM International, (2015), 45–46

[9] Yamauchi K., Ohkata I., Tsuchiya K., Miyazaki S. (eds.): Shape Memory and Superelastic Alloys: Technologies and Applications. In: Woodhead Publishing Series in Metals and Surface Engineering. Woodhead 2011

[10] PN-EN 10088-1:2014-12 Stale odporne na korozję – Część 1: Wykaz stali odpornych na korozję

[11] Active Standard ASTM A240/A240M, Standard Specification for Chromium and Chromium-Nickel Stainless Steel Plate, Sheet, and Strip for Pressure Vessels and for General Applications

[12] Terpiłowski J., Panas A.J., Majewski T.: Badania dyfuzyjności cieplnej materiału fazy wiążącej spieku 90W-7Ni-3Fe. Biuletyn WAT, vol. LVIII, nr 2 (2009), 363–375

[13] Panas A.J., Terpiłowski J., Majewski T.: Badania i analiza właściwości cieplno-fizycznych spieku 90W-7Ni-3Fe. Biuletyn WAT, vol. LIX, nr 3 (2010), 361–380

[14] Terpiłowski J.: A pulse method for determining the thermal diffusivity of solids by measuring the temperature difference between the extreme surfaces of the sample. Journal of Technical Physics, 25, 3–4 (1984), 429–439